

# Cytoskeletal track selection during cargo transport in spermatids is relevant to male fertility

Abraham L. Kierszenbaum,\* Eugene Rivkin and Laura L. Tres

Department of Cell Biology and Anatomy; The Sophie Davis School of Biomedical Education; The City University of New York; New York, NY USA

**Key words:** manchette, acrosome, acroplaxome, sperm head shaping

Spermatids generate diverse and unusual actin and microtubule populations during spermiogenesis to fulfill mechanical and cargo transport functions assisted by motor and non-motor proteins. Disruption of cargo transport may lead to teratozoospermia and consequent male infertility. How motor and non-motor proteins utilize the cytoskeleton to transport cargos during sperm development is not clear. Filamentous actin (F-actin) and the associated motor protein myosin Va participate in the transport of Golgi-derived proacrosomal vesicles to the acrosome and along the manchette. The acrosome is stabilized by the acroplaxome, a cytoskeletal plate anchored to the nuclear envelope. The acroplaxome plate harbors F-actin and actin-like proteins as well as several other proteins, including keratin 5/Sak57, Ran GTPase, Hook1, dynactin p150Glued, cenexin-derived ODF2, testis-expressed profilin-3 and profilin-4, testis-expressed Fer tyrosine kinase (FerT), members of the ubiquitin-proteasome system and cortactin. Spermatids express transcripts encoding the non-spliced form of cortactin, a F-actin-regulatory protein. Tyrosine phosphorylated cortactin and FerT coexist in the acrosome-acroplaxome complex. Hook1 and p150Glued, known to participate in vesicle cargo transport, are sequentially seen from the acroplaxome to the manchette to the head-tail coupling apparatus (HTCA). The golgin Golgi-microtubule associated protein GMAP210 resides in the cis-Golgi whereas the intraflagellar protein IFT88 localizes in the trans-Golgi network. Like Hook1 and p150Glued, GMAP210 and IFT88 colocalize at the cytosolic side of proacrosomal vesicles and, following vesicle fusion, become part of the outer and inner acrosomal membranes before relocating to the acroplaxome, manchette and HTCA. A hallmark of the manchette and axoneme is microtubule heterogeneity, determined by the abundance of acetylated, tyrosinated and glutamylated tubulin isoforms produced by post-translational modifications. We postulate that the construction of the male gamete requires microtubule and F-actin tracks and specific molecular motors and associated non-motor proteins for the directional positioning of vesicular and non-vesicular cargos at specific intracellular sites.

## Introduction

Spermatids are highly polarized cells. Their polarity is determined by the opposite position of the Golgi-acrosome-acroplaxome complex and the head-tail coupling apparatus (HTCA) with respect to the nucleus. Central to the development of polarity are two cargo transport pathways: an intramanchette transport (IMT) pathway<sup>1</sup> and an intraflagellar transport (IFT) pathway (for a review see ref. 2) (Fig. 1). IMT is transient as the manchette itself; it is involved in the trafficking of cargos between the nucleus and the cytoplasm and to the HTCA. IFT participates in the development of the future sperm tail. In general, IMT and IFT share similar cytoskeletal tracks and motor and non-motor proteins. Two cytoskeletal components, actin-containing microfilaments (F-actin) and microtubules, provide tracks for IMT and IFT. How IMT and IFT operate during spermiogenesis is the focus of continuing research. The basic premise is that molecular motors and non-motor proteins utilize F-actin and microtubule tracks to deliver vesicular and non-vesicular cargos to appropriate intracellular domains in spermatids. A number of mutant mouse models demonstrate that a disruption in the delivery of cargos to the appropriate assembly site in spermatids seriously affects sperm development. Yet, experimental approaches are needed to better understand how molecular motors in spermatids recognize specific cytoskeletal tracks and target selected cargos to specific subcellular sites.

The Golgi apparatus, one of the milestones of spermatid polarity, is the source of proacrosomal vesicles transported along microtubules and F-actin to the acroplaxome where they tether and fuse to form first the acrosome vesicle and later the acrosome sac.<sup>3,4</sup> Soon after acrosome biogenesis starts, a transient and predominant microtubule manchette develops at the caudal site of the acrosome-acroplaxome complex. F-actin is also present in the manchette.<sup>5</sup> The acroplaxome is an F-actin-keratin 5/Sak57-containing cytoskeletal plate similar to the perinuclear theca<sup>6</sup> except for an unconventional desmosome-like marginal ring (Fig. 2). The marginal ring fastens the descending recess of the acrosome sac to a shallow indentation of the nuclear envelope-dense nuclear lamina complex.<sup>3</sup> A spermiogenesis-specific LINC complex (for linker of nucleoskeleton and cytoskeleton) bridges the dense nuclear lamina to F-actin in the acroplaxome.<sup>7</sup> As a result, the acroplaxome not only stabilizes the acrosome during

\*Correspondence to: Abraham L. Kierszenbaum; Email: kier@med.cuny.edu  
Submitted: 08/15/11; Accepted: 09/06/11  
<http://dx.doi.org/10.4161/spmg.1.3.18018>

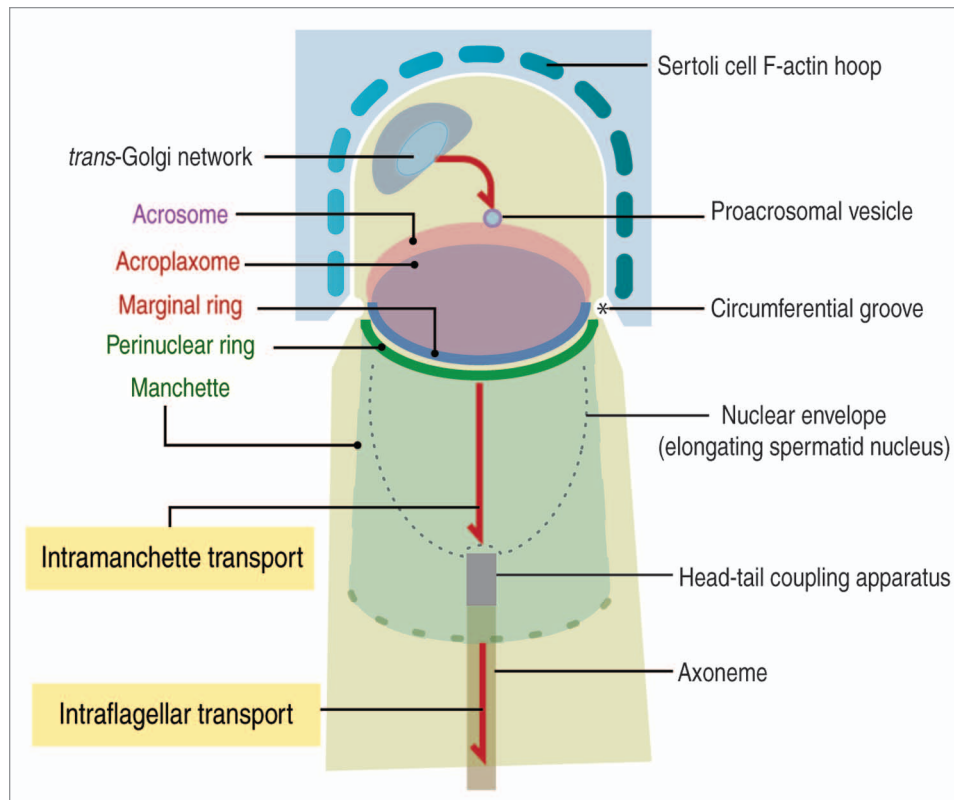


**Figure 1.** Diagrammatic representation of the cargo transport pathways in spermatids. A trans-Golgi—to acrosome pathway, involving F-actin and microtubules tracks, leads Golgi-derived proacrosomal vesicles to the acrosome. Two structural elements are illustrated: an acroplaxome plate, surrounded by a marginal ring anchoring the acrosome to the spermatid nuclear envelope and a temporary manchette, consisting of a perinuclear ring and inserted microtubules. The acroplaxome marginal ring and the manchette perinuclear ring are opposite to each other at the circumferential groove zone. The manchette contains motor and non-motor proteins involved in intramanchette transport and nucleocytoplasmic exchange.<sup>10</sup> The head-tail coupling apparatus (HTCA) connects the elongating spermatid head to the axoneme, a component of the developing tail. Combined intramanchette and intraflagellar transport pathways participate in the development of the HTCA and the tail with the contribution of motor and non-motor proteins, including members of the intraflagellar transport (IFT) protein family. Microtubules of the manchette and axoneme consist of tubulin subunits with post-transcriptional modifications (acetylation, tyrosination and glutamylation).<sup>46</sup> Sertoli cell F-actin-containing hoops embrace the apical region of the elongating spermatid up to the circumferential groove.

its biogenesis but also anchors the acrosome to the spermatid cortical nucleoskeleton during head shaping. It also provides a temporary niche for proteins in transit to the manchette, and places proteins close to a spermatid nuclear region where condensation and transcriptional silencing start. As the biogenesis of the acrosome-acroplaxome-manchette complex is in progress, microtubules and associated proteins with functional requirements in spermiogenesis—including keratin 5/Sak57,<sup>3</sup> GMAP210,<sup>8</sup> IFT88,<sup>8</sup> Hook1,<sup>9</sup> Ran GTPase<sup>10</sup> and ODF2,<sup>11</sup> and components of the ubiquitin-proteasome system<sup>12</sup>—are transported to specific sites to transform a round spermatid into a self-propelling sperm.

There is a remarkable aspect of the manchette and axoneme: their microtubules contain abundant post-translationally modified tubulin subunits. In somatic cells and during neuronal axonal transport of neurotransmitters, different protein motors select diverse subpopulations of post-translationally modified microtubules to partition the transport of cargos so they can reach specific intracellular sites.<sup>13</sup> This aspect needs to be explored in spermatids. Here, we review and integrate recent findings concerning the transport of Golgi-derived proacrosomal vesicles to

the acrosome-acroplaxome complex and the regulatory dynamics of F-actin in the acroplaxome, including the expression of cortactin transcripts in spermatids. We highlight the consistent acroplaxome-to-manchette-to HTCA sequential redistribution of several proteins and add two proteins to an enlarging catalog: Hook1, a protein that binds vesicle cargos to microtubules, and dynactin (p150<sup>Glued</sup>), a member of a protein complex that associates with cytoplasmic dynein during the transport of vesicle cargos along microtubules.

### The Golgi, the Origin Site of Vesicular Cargos Transported along F-Actin and Microtubules Tracks

Like in somatic cells, the spermatid Golgi consists of stacks of closely apposed flattened membrane discs, the Golgi ribbon, flanked by a cytomembrane network that serves as a cargo entry (cis-Golgi) site and a trans-Golgi network (TGN) distribution site of proacrosomal vesicles. The fine structure and function of the spermatid Golgi have been reviewed in reference 6. The association of microtubules with the Golgi in spermatids has

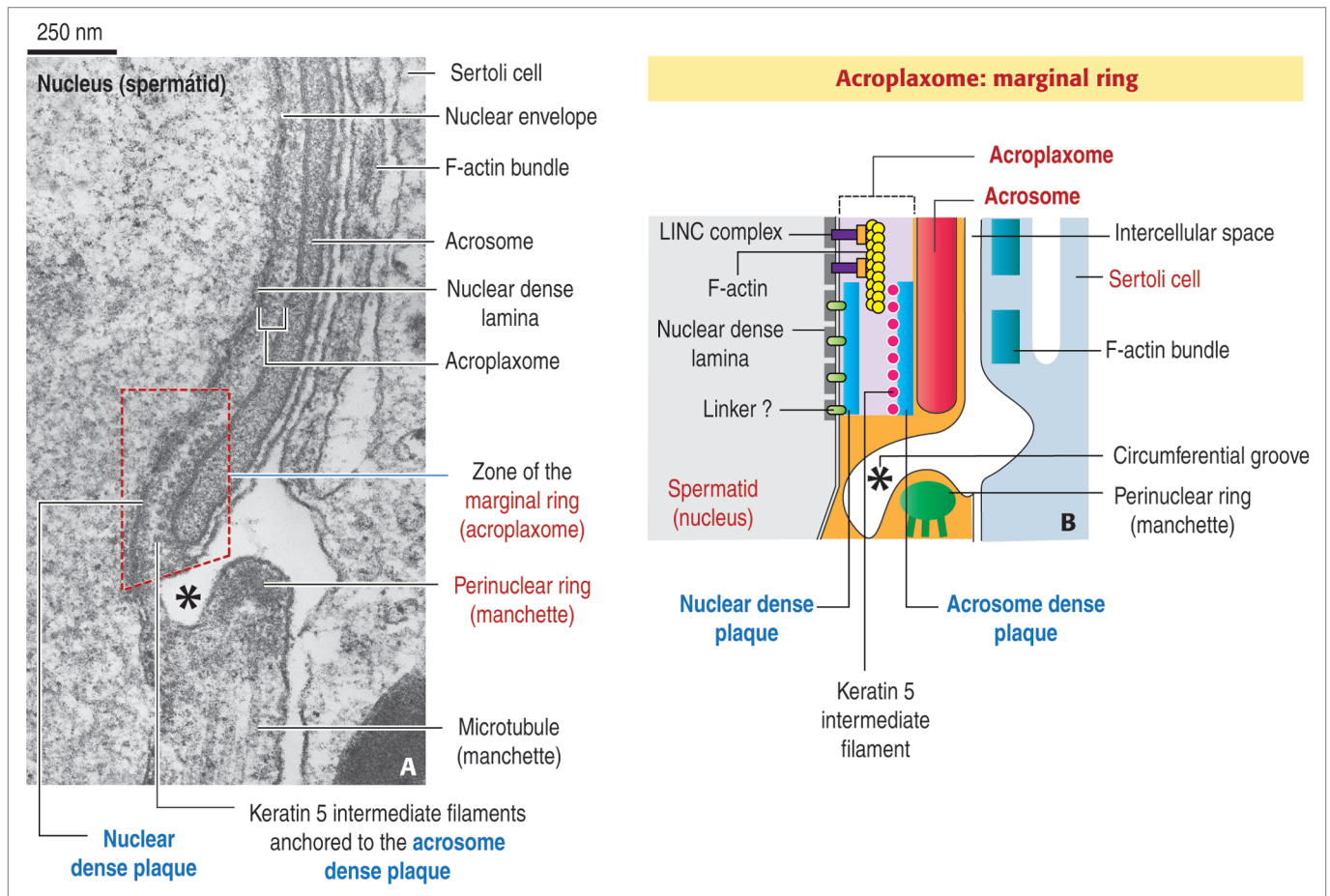


**Figure 2.** Diagrammatic representation of the marginal ring of the acroplaxome. (A) The electron micrograph illustrates the opposite acroplaxome marginal and manchette perinuclear rings at the circumferential groove region (asterisk). The marginal ring (red dashed box) consists of a nuclear dense plaque associated with the nuclear dense lamina of the spermatid nucleus, just under the nuclear envelope, and an acrosome dense plate attached to the inner acrosome membrane at the caudal recess of the acrosome. Keratin 5/Sak57-containing intermediate filaments are attached to the acrosome dense plaque. F-actin bundles in the adjacent Sertoli cell align along a flat cisterna and span up to the circumferential groove region. (B) The diagram (not to scale) illustrates the same component of the acroplaxome marginal ring shown in (A). A LINC protein complex<sup>7</sup> extends from the nuclear dense lamina to F-actin in the acroplaxome plate, just above the marginal ring. Additional linkers may connect the nuclear dense lamina to the nuclear dense plaque.

been documented by immunofluorescence microscopy.<sup>14</sup> The blocking effect of nocodazole and Brefeldin A on microtubule-based transport of Golgi-derived proacrosomal vesicles to the acrosome-acroplaxome complex has been reported in reference 8. Proacrosomal vesicles utilize two different routes to reach the acrosome: a F-actin route, involving the motor myosin Va linked to melanophilin, an adaptor connected to vesicle-bound Rab27a/b,<sup>4,5</sup> and a microtubule route, involving members of the kinesin-2 motor protein family, including the KIFC1 variant.<sup>15</sup>

More recently, it was shown that the golgin GMAP210 (for Golgi microtubule associated protein with a molecular mass of 210 kDa<sup>16</sup>) resides in the cis-Golgi of spermatids and is involved in proacrosomal vesicle transport.<sup>8</sup> In somatic cells, GMAP210 is necessary for maintaining the integrity of the Golgi ribbon.<sup>17,18</sup> GMAP210 co-purifies with microtubules,<sup>19,20</sup> interacts with centrosomal  $\gamma$ -tubulin,<sup>17</sup> and when overexpressed perturbs the organization of the microtubule network.<sup>19</sup> The C-terminal region of GMAP210 contains a GRAB domain (for GRIP-related Arf

binding domain<sup>21</sup>) that specifically binds flat membranes in an Arf1-dependent manner in *in vitro* assays.<sup>22</sup> The N-terminal region contains an ALPS (for amphipathic lipid-packing sensor) motif sensitive to membrane curvature.<sup>22</sup> The structural characteristics of the GRAB and ALPS terminal domains and a hinge region in the coiled-coil region of GMAP210 have led to an *in vitro* model in which membranes of spherical and flat curvature bind respectively to the N- and C-terminus of GMAP210.<sup>22</sup> This model may predict that GMAP210 captures spherical proacrosomal vesicles and links them to the outer acrosome membrane where membrane fusion occurs. The hinge region may facilitate the apposition of membranes to converge and fuse. Two issues arise: Does this *in vitro* vesicle capture model operate *in vivo* in spermatids? If so, how do vesicles link to microtubules for vesicle transport toward the acrosome and by IMT to the HTCA? Following proacrosomal vesicle fusion, GMAP210 is seen along the outer and inner acrosome membranes. Thus, Golgi-derived proacrosomal vesicles not only deliver acrosomal proenzymes but

also supply membrane-associated GMAP210 as well as other proteins to the acrosome sac. Additional proteins include IFT88, testis-expressed FerT tyrosine kinase;<sup>23</sup> Fyn tyrosine kinase;<sup>24</sup> and members of the ubiquitin-proteasome system.<sup>12</sup> Whether these and other proteins utilize the acrosome membrane pathway to contribute to acrosome biogenesis and also as a strategy to reach a juxtannuclear niche position to participate in nuclear condensation and transcriptional inactivation need to be explored.

Cargos are mobilized along microtubules of the axoneme by the kinesin-2 motor (also known as the KIF3 motor complex) together with proteins of the intraflagellar transport-A (IFT-A) and IFT-B complexes.<sup>2</sup> Proteins of the IFT-B class are essential for anterograde cargo trafficking (toward the plus-end of a microtubule) whereas IFT-A and cytoplasmic dynein are required for retrograde trafficking (towards the minus-end of a microtubule). IFT88 is a member of the IFT-B protein complex. In contrast to the localization of GMAP210 in the cis-Golgi, IFT88 exists in the TGN. At the TGN, both proteins co-localize on the cytosolic side of proacrosomal vesicles and coexist along the outer and inner acrosome membranes, the HTCA, and the developing tail.<sup>8</sup> IFT20, another member of the IFT-B complex also seen in the Golgi and manchette of spermatids,<sup>25</sup> interacts in the Golgi of somatic cells with a specific GMAP210 domain at the coiled-coil region.<sup>26</sup> Whether GMAP210 and IFT88 interact with each other needs to be determined. Yet, a significant observation is the coexistence of two members of the IFT-B class, IFT20 and IFT88, in the Golgi of spermatids.

Microtubules and their associated kinesin-2 and cytoplasmic dynein motors and non-motor proteins have been linked to cargo trafficking at the Golgi and from the Golgi to the acrosome.<sup>15,27</sup> There is evidence that the actin-based motor myosin Va, interacting with Rab27a/Rab27b in proacrosomal vesicles, also participates in acrosome biogenesis.<sup>4,5</sup> The issue before us is to determine why two classes of cytoskeletal cargo transport systems are needed during spermatid development. This also raises the questions of whether multiple motors are required to move a single cargo over distances of several micrometers in such a way that when the first motor detaches the second motor maintains attachment to a cytoskeletal track<sup>28</sup> and whether switching between heterogeneous cytoskeletal tracks (from actin to microtubules to actin) is facilitated by the coexisting motor myosin Va on the same cargo.<sup>29</sup> A combination of the two cytoskeletal tracks would successfully contribute to the long-range (on microtubules) or short-range (on actin) delivery of cargos to three essential sites: the acrosome-acroplaxome complex, the HTCA (by IMT), and the developing spermatid tail (by IFT).

The *Ift88* mutant mouse expresses defective IFT88 but has an intact actin-based myosin Va-Rab27a/Rab27b vesicle transport system.<sup>8</sup> The *Ift88* mutant mouse is a convenient model for analyzing the role of the protein IFT88 during spermatid development because of a combined defect in IMT and IFT results in the production of tail-less spermatids.<sup>8</sup> The development of the acrosome-acroplaxome complex is not significantly disrupted in the *Ift88* mutant. Yet, the actin-based transport system does not offset the deficiency of the microtubule-based transport system

caused by non-functional IFT88 protein. Like myosin Va and Rab27/Rab27b, GMAP210 and IFT88 appear to participate in the IMT of cargos to the HTCA and the tail. It appears that cargo transport along microtubule tracks takes dominance in tail development in the *Ift88* mutant mouse.

### Acroplaxome, a Cytoskeletal Structure Involved in Acrosome Biogenesis and Spermatid Head Shaping

The acroplaxome<sup>3</sup> consists of an F-actin-keratin 5/Sak57—containing cytoskeletal plate limited by a marginal ring. The marginal ring is anchored to a shallow indentation of the nuclear envelope by a desmosome-like structure consisting of two dense plaques: an acrosomal dense plaque anchored to the inner acrosome membrane, and a nuclear dense plaque attached to the nuclear envelope (Fig. 2A and B). The plate portion is secured to the spermatid nucleus by a spermiogenesis-specific LINC complex extending from the subjacent dense nuclear lamina and linked to F-actin.<sup>7</sup>

Two functions have been ascribed to the acroplaxome. First, Golgi-derived proacrosomal vesicles tether, dock and fuse along the incipient acroplaxome plate to form first the acrosome vesicle and later the acrosome sac.<sup>3</sup> Second, F-actin and keratin 5/Sak57 provide the acroplaxome with the ability to modulate clutching forces originated in Sertoli cell F-actin hoops embracing the elongating spermatid head.<sup>30</sup> Acroplaxome flexibility requires the dynamic reorganization of F-actin and keratin 5/Sak57. Cortactin, a protein that interacts with the actin nucleator Arp 2/3 complex, regulates the arrangement of F-actin network when phosphorylated by protein kinases.<sup>31</sup> Cortactin, assumed to be expressed only by Sertoli cells in testis, is encoded by the *Cttn* gene, whose abnormal expression correlates with elongated spermatids displaying abnormal head shape and premature detachment of round spermatids from Sertoli cell niches.<sup>32</sup> Figure 3 documents the expression of cortactin transcripts in round spermatids. Two forms of cortactin are expressed in rat: a spliced form, encoding 5.5 cortactin repeats, and a non-spliced form, encoding 6.5 cortactin repeats. Rat testis, including round spermatids, express the non-spliced form of cortactin. Tyrosine phosphorylated cortactin is seen in the acroplaxome while non-phosphorylated cortactin predominates in the manchette.<sup>23</sup> Phosphorylated cortactin in the acroplaxome and in the F-actin-containing Sertoli cell hoops suggests a combined Sertoli cell hoop-acroplaxome mechanical role of microfilaments in spermatid head shaping.<sup>3,30</sup>

Phosphorylated cortactin coexists with FerT, the testicular form of the somatic non-receptor protein tyrosine kinase Fer, designated FerS.<sup>23</sup> FerS contains an amino-terminal FCH (for Fps/Fes/Fer/CIP4 homology) domain implicated in the regulation of cytoskeletal rearrangements and vesicular transport. The FCH domain is not present in FerT. Instead, a unique 44-amino acid amino terminal sequence is observed.<sup>23</sup> This difference suggests that FerS and the FerT can bind to distinct substrates with diverse biological function, a possibility highlighted by prevalence of FerT in pachytene spermatocytes and round spermatids. The coexistence of FerS, although at a low level, and FerT transcripts in pachytene spermatocyte suggests that the two forms of

Fer are required during meiotic prophase. This does not seem to be the case in round spermatids where FerS is not detected.

In addition to Fer tyrosine kinase, Fyn tyrosine kinase has also been associated with cortactin phosphorylation in somatic cells.<sup>31,33</sup> There are specific structural features of testicular Fyn tyrosine kinase to highlight. Full-length and truncated transcripts of Fyn tyrosine kinase are expressed during testicular development.<sup>24</sup> Truncated Fyn (designated tr-Fyn) transcripts encode a 24 kDa protein with a N-terminal domain, a complete Src homology (SH) 3 domain and an incomplete SH2 domain. The kinase domain is missing in tr-Fyn. Surprisingly, spermatids express tr-Fyn transcripts and protein, but not full-length Fyn transcripts and protein. In contrast, Sertoli cells express full-length and truncated Fyn throughout testicular development. Sperm contain full-length Fyn transcripts and protein but not the truncated form. Like FerT, tr-Fyn protein is visualized at the cytosolic side of TGN-derived proacrosomal vesicles, along the outer acrosome membrane and the inner acrosome membrane-acroplaxome site. Since tr-Fyn is devoid of a tyrosine kinase domain, it is likely that SH3 and SH2 domains may perform kinase-independent functions at their diverse localization sites.

The striking number of actin-related and actin-like proteins expressed in testis and spermatids in particular is rather intriguing. For example, actin-related proteins Arp1;<sup>34</sup> Arp-T1/Arp-T2<sup>35</sup>; testis actin-like proteins [mouse Tact1/Tact2;<sup>36</sup> mouse T-ACTIN 1 and T-ACTIN 2;<sup>37</sup> human actin-like 7A (ACTL7B) and actin-like 7A (ACTL7A)<sup>38</sup>] and actin-capping proteins (rat<sup>39</sup>) have been reported in spermatids. ACTL7A in human and the equivalent Tact2 and T-ACTIN2 proteins in mouse are testis-specific actin-related proteins, which may play a role in actin dynamics by interacting with specific binding protein partners.<sup>40</sup> Another example is the expression in spermatids of profilin 3 and profilin 4, wherein profilin-3, but no profilin-4, interacts with actin.<sup>41</sup> Most members of the profilin family sequester monomeric actin (G-actin) from the actin pool and catalyze the exchange of actin-bound ADP to ATP to facilitate actin polymerization. Profilin also has high binding affinity for proline-rich proteins, such as cortactin. Given the striking expression of subsets of actin-related proteins, tubulin isoforms and truncated tyrosine kinases in spermatids, it is likely that testis-specific transcription factors, alternative transcription initiation sites and developmentally regulated post-translational processing could drive the expression of uncommon cytoskeletal homologues and truncated tyrosine kinases (such as FerT) to fulfill new functions or the modulation of existing functions compatible with spermatid differentiation and survival.

### Hook1 and p150Glued Relocate from the Acrosome-Acroplaxome Complex to the Manchette to the HTCA

Hook1 is a member of Hook family of coiled-coil proteins with binding affinity to microtubules and cargos through the N- and C-terminal domains, respectively.<sup>42</sup> In spermatids, Hook1 is initially detected in the TGN, in association with Golgi-derived proacrosomal vesicles (Fig. 4A–F and M). Like GMAP210,

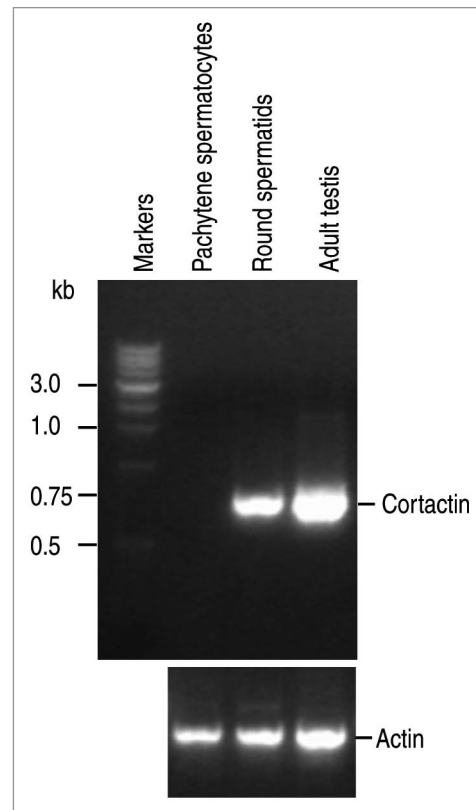


**Figure 3.** RT-PCR analysis of cortactin transcript expression. Cortactin transcripts are seen in rat round spermatids and adult rat testis but not in rat pachytene spermatocytes. The following primers were used: Cortactin-Forward 1<sub>283</sub> ATC GGG GCA CCA GGA ACA CAT CAA<sub>306</sub>; Cortactin-Reverse 1<sub>1029</sub> GAC GGC ACC TGG ACC ACT TCT TCA<sub>1005</sub>; Five isoforms of cortactin are expressed in mice; two isoforms of cortactin are expressed in rat and *Xenopus*; and three isoforms of cortactin are expressed in human. The primers were selected to span a stretch of 111 bp cDNA (spliced from some transcripts) to determine which cortactin form is expressed in spermatogenic cells and testis. The spliced sequence corresponds to nucleotides 864–974. The expected sizes of the fragments were 746 bp for the not spliced form and 635 bp for the spliced form. The transcript form expressed in round spermatids and testis is the non-spliced form. Actin primers were used as control. The construction of rat pachytene spermatocyte and round spermatid cDNA libraries was reported in reference 49.

Hook1 becomes part of the outer and inner acrosomal membranes following fusion of proacrosomal vesicles with the acrosome sac. When spermatid elongation starts, Hook1 relocates from the acrosome-acroplaxome complex to the manchette. After manchette disassembly, Hook1 is seen at the HTCA (Fig. 4J–L). The significance of Hook1 in spermatid development is based on the expression of a truncated form of Hook1 in the *azh* mutant mouse,<sup>9</sup> displaying sperm with abnormal head shape, head dislocation and tail coiling.<sup>43</sup> An antibody produced against a peptide located in the C-terminal region of Hook1 recognizes full-length Hook1 but does not recognize the truncated form expressed in the testis of *azh* mutant mouse (Fig. 4N). Hook1 emerges as a candidate protein transported to the HTCA by IMT to stabilize the attachment of the sperm head to the tail and the organization of the tail. Yet, the precise function of Hook1 is still undetermined.

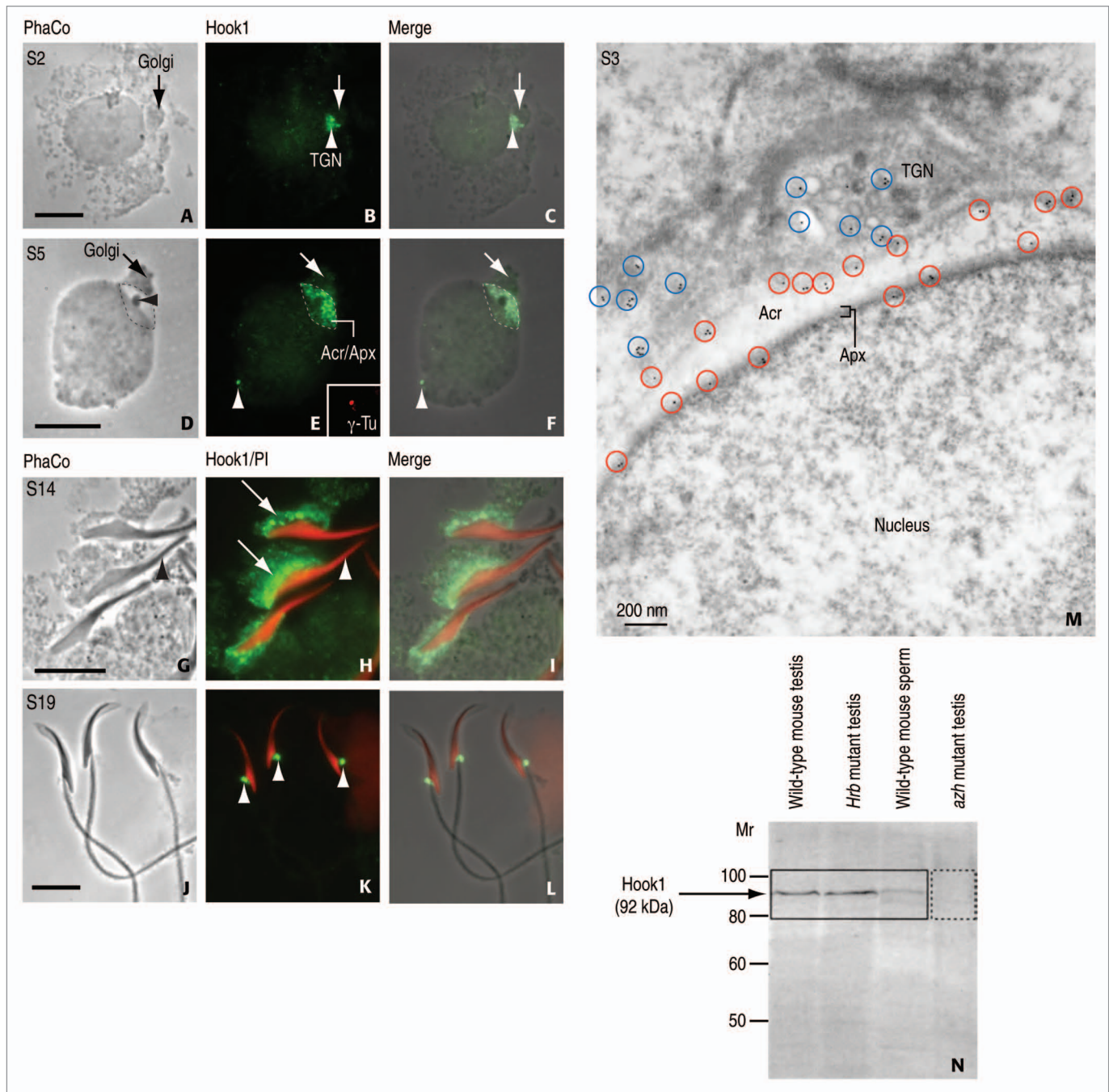
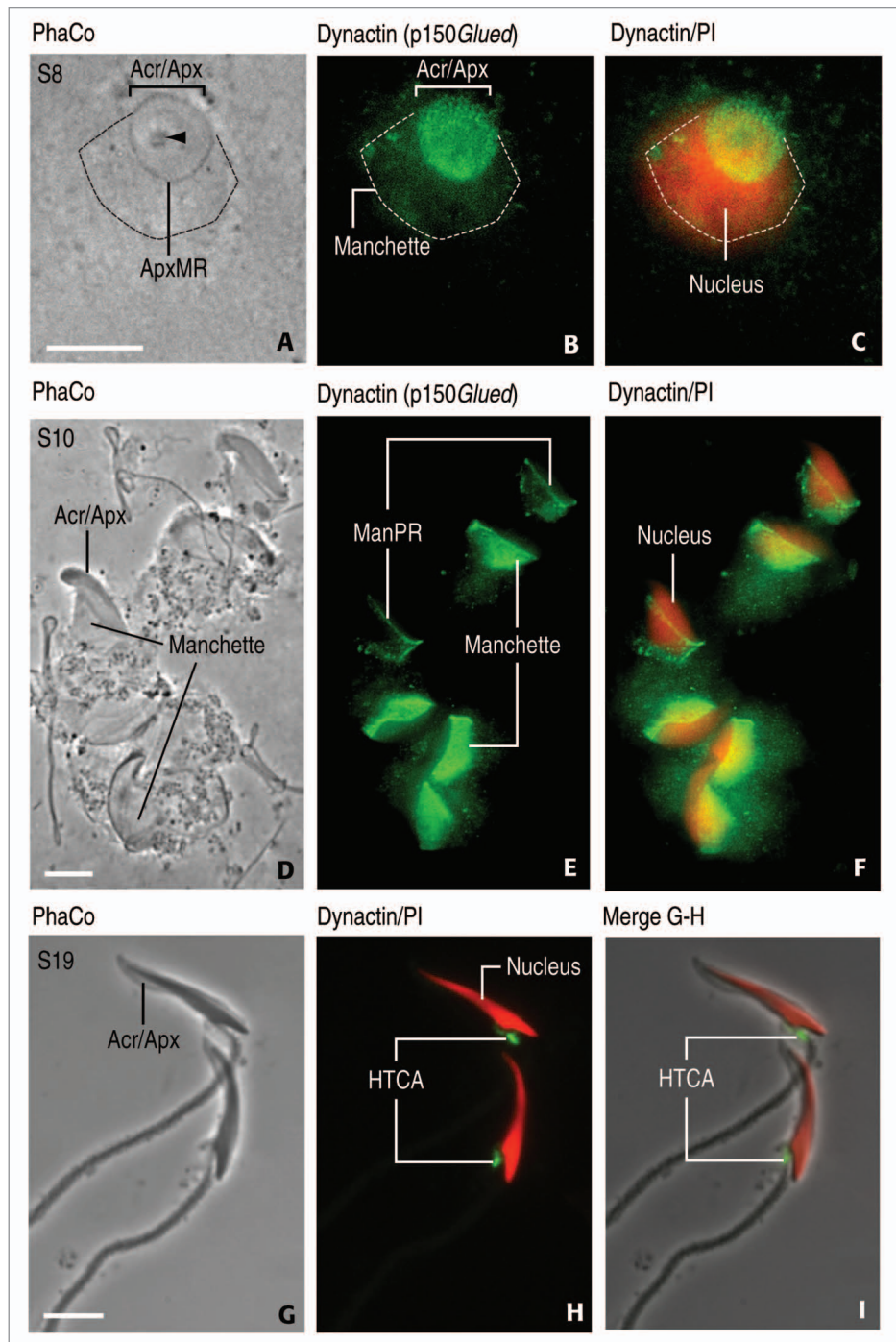


**Figure 4.** Immunocytochemical localization and immunoblotting of Hook1. (A, D, G and J) are phase-contrast (PhaCo) microscopy. (A–C) (step 2 of spermiogenesis; S2): Hook1 immunoreactive sites are seen at the trans-Golgi network (TGN, white arrowhead in B) and the acrosome-acroplaxome of a rat round spermatid. The arrows in (A–C) indicate the Golgi. (C) is the merge of (A and B). (D–F) (S5): Hook1 is predominantly located at the acrosome-acroplaxome (Acr/Apx) region and in the centriolar region opposite to the acrosome (white arrowhead in E and F). The inset in (E) corresponds to a double staining with  $\gamma$ -tubulin (SIGMA, St. Louis, MO; working dilution: 1:50; catalog number T6557) to confirm the localization of Hook1 in the centrosome. The arrows in (D–F) indicate the Golgi. (F) is the merge of (D and E). (G–I) (S14): Hook1 is localized in the manchette (arrows in H) of elongating spermatids. No immunoreactivity is seen in the acrosome-acroplaxome region (arrowhead in G and H). PI denotes nuclear red staining with propidium iodide. (I) is the merge of (G and H). (J–L) (S19): Hook1 is seen in the HTCA (arrowheads in K) of mature spermatids. (L) is the merge of (J and K). (M) (S3): Immunogold electron microscopic localization of Hook1 in a rat round spermatid. The blue circles denote immunoreactive sites at the TGN region, mainly at the cytosolic side of proacrosomal vesicles. The red circles indicate the localization of Hook1 along the outer acrosomal membrane and at the inner acrosome membrane-acroplaxome (Apx) interface. Acr: acrosome. (N) Immunoblot showing the immunoreactive 92 kDa (729 amino acids) Hook1 protein in wild-type mouse testis, the acrosome-less *Hrb* mutant mouse testis, and wild-type mouse sperm but not in testis from the *azh* mutant, known to express truncated Hook1 lacking the C-terminus. Affinity purified polyclonal antibody was generated in rabbit using as antigen the peptide  $_{625}$ RNV IKT LDP KLN PAS $_{639}$  corresponding to the C-terminal region of Hook1 (mouse; GeneBank Acc. No. AF487912). Hook1 antibody working dilution of 1:100 was used for indirect immunofluorescence and 1:25 for immunogold electron microscopy carried out according to previously reported procedures in reference 8. Scale bars in (A, D, G and J) 5  $\mu$ m.

**Figure 5.** Localization of dynactin (p150*Glued*) in rat spermatids by indirect immunofluorescence. (A, D and G) are phase-contrast (PhaCo) microscopy (A–C) (step 8, S8): Immunoreactivity is concentrated in the acrosome-acroplaxome complex (top view; Acr/Apx) of a rat spermatid. Specific immunoreactivity is seen in the manchette, whose perimeter is indicated by a dashed line in (A–C). The arrowhead in (A) indicates the acrosome granule in the acrosome overlapping the acroplaxome. The bracket indicates the width of the acrosome-acroplaxome (Acr/Apx) complex. The marginal ring of the acroplaxome (ApxMR) is pointed in (A). (C) illustrates a spermatid nucleus (stained red with propidium iodide, PI) partially overlapped by the manchette. (D–F) (S10): Elongating rat spermatid showing dynactin (p150*Glued*) in the manchette. A distinct linear staining at the perinuclear ring of the manchette (ManPR) of two spermatids suggests the primary accumulation of the antigen. At this step, there is no immunostaining at the Acr/Apx region. (F) indicates dynactin/PI combined staining. (G–I) (S19): Mature rat spermatids display dynactin (p150*Glued*) in the HTCA. No specific staining is seen at the Acr/Apx region (denoted in G). The manchette has already disassembled at this spermiogenic step. (I) is a merge of (G and H). Spermatid nuclei are stained red with PI. Dynactin antibody was from Santa Cruz Biotechnology [Santa Cruz, CA; catalog number sc-9801; affinity purified goat polyclonal antibody raised against a peptide corresponding to the C-terminus of human dynactin 1 (C-20)]. The antiserum detects the p150*Glued* splice variant (rat, mouse, human). Working dilution: 1:100; second antibody was Alexa Fluor-conjugated anti-goat (working dilution, 1:200; Molecular Probes, Eugene, OR). Specimens were mounted with Vectashield (Vector Laboratories, Burlingame, CA) without or with propidium iodide (to detect nucleic acids by a red emission color). Scale bars in (A, D and G): 5  $\mu$ m.



Hook1 is encoded by 22 exons. The protein consists of a microtubule-binding domain at the N-terminus, a central coiled-coil homodimerization domain and a vesicle-binding domain at the C-terminus. Exons 10 and 11, which are encoding parts of the coiled-coil and the vesicle-binding domains, are deleted in the *azh* mutant mouse. This causes a disruption in the reading frame and results in the production of a truncated protein. It is not known whether the missing C-terminal domain is necessary for additional proteins to bind during cargo transport (such as members of the Rab protein family present on the surface of transporting vesicles<sup>4,5,30</sup>), or is essential for homodimerization.

It is possible that the microtubule-binding domain of dimerized Hook1 may stabilize the “tube-like” or “intertube-like” microtubule assembly of the manchette<sup>5,30</sup> to enable undisturbed cargo trafficking.

Dynactin is a multisubunit protein complex which associates with cytoplasmic dynein, a motor protein that binds to microtubules during vesicular cargo transport. The dynactin subunit, p150*Glued*, is capable of microtubule-cytoplasmic dynein interaction leading to the transport of vesicular cargos.<sup>44</sup> Like GMAP210, IFT88 and Hook1, p150*Glued* reaches the acrosome-acroplaxome complex (Fig. 5A–D), and then is visualized in the

manchette (Fig. 5D–F) and later in the HTCA (Fig. 5G–I). In several manchettes, p150<sup>Glued</sup> immunoreactivity aligns along the perinuclear ring of the manchette, suggesting a molecular motor front or reservoir (see Fig. 5E). It is striking that several proteins involved in cargo transport display a similar sequential distribution: from the cytosolic surface of Golgi-derived proacrosomal vesicles to the acrosome-acroplaxome complex to the manchette to the HTCA. The challenge is to determine whether motor and non-motor proteins act independently or synergistically to segregate cargos during spermatid morphogenesis and whether motor proteins have preference for microtubules marked by post-translationally modified tubulins for cargo trafficking. Added to this challenge is the coexistence of F-actin and microtubule tracks, each served by specific motor proteins. These are important areas for further studies in light of significant sperm aberrations in mutants mice associated with defective IMT and IFT during sperm development.

### IMT, a Transient Cargo Transporting Route to the HTCA and Tail

In contrast to the acroplaxome, the manchette is a temporary structure consisting of a dense perinuclear ring and inserted microtubules. The perinuclear ring of the manchette assembles caudally and proximal to the marginal ring of the acroplaxome. Four relevant aspects define the topography of the manchette. First, the manchette assembles soon after the desmosome-like marginal ring of the acroplaxome starts to organize. Second, a circumferential groove specifies the boundary between the overlapping marginal ring of the acroplaxome and perinuclear ring of the manchette. Third, the circumferential groove marks the end point of Sertoli cell-derived F-actin hoops embracing the elongating spermatid head (see Fig. 2A and B). Fourth, the manchette is strategically located at the nucleo-cytoplasmic interchange crossroad involving the Ran GTPase machinery.<sup>10</sup> Sertoli cell hoops are not visualized below the groove region. Consequently, the upper portion of the elongating spermatid head, containing the acrosome-acroplaxome complex, is under surveillance of the Sertoli cell F-actin clutch. In contrast, the lower portion of the elongating head is embraced by the predominantly microtubule-containing manchette. Essentially, the elongating spermatid head is partitioned into two distinct domains by two different cytoskeletal components: the F-actin-keratin 5/Sak57-containing acroplaxome and the microtubule-containing manchette, respectively. It is at this boundary that the marginal ring of the acroplaxome and the perinuclear ring of manchette behave similarly: they gradually reduce their diameter to conform, in a sleeve-like fashion, with the narrowing of the elongating spermatid nucleus. Asynchronous ring diameter-nuclear reduction in mutants results in a “strangling” zone at the rings’ site, an indication of abnormal head shaping.<sup>3</sup>

The microtubule mantle lengthens caudally from the perinuclear ring and houses microtubule-based kinesin and cytoplasmic dynein motors.<sup>45</sup> Fractionated manchettes and axonemes from spermatids and sperm of wild-type and *azh* mutant mice<sup>43</sup> display substantial microtubule heterogeneity characterized by specific post-translational modifications of tubulin subunits

$\alpha$  and  $\beta$  (reviewed in ref. 46). These modifications include acetylation of  $\alpha$ -tubulin, removal of the terminal tyrosine residue from  $\alpha$ -tubulin (detyrosination), and addition of variable length chains of glutamate residues to  $\alpha$ -tubulin and  $\beta$ -tubulin (glutamylolation). Acetylated tubulin is more abundant in manchettes than in epididymal sperm axonemes whereas tyrosinated tubulin is reduced in manchettes and axonemes. No relevant biochemical bulk differences exist in manchette and axoneme derived from wild-type and *azh* mutant mice despite the existence of severe alteration in sperm head shape, dislocation at the sperm HTCA and tail coiling.<sup>43</sup> Yet, the distribution within the manchette of microtubule heterogeneous populations remains to be determined. There is a need to map manchette microtubule heterogeneity by imaging techniques and evaluate whether molecular motor and non-motor protein may decode microtubule diversity into function. These aspects can be initially studied in vitro using fractionated manchettes from spermatids treated in vitro with pharmacologic agents affecting cytoskeletal dynamics<sup>8</sup> as well as by simultaneous imaging of motors/non-motor proteins and cytoskeletal track to account for shifts in their position with respect to subsets of microtubules.

### Concluding Remarks

Although the presence and arrangement of microtubules and microfilaments in spermatids have been known for many years, the cargo transporting function of the manchette has only recently begun to be considered.<sup>1</sup> Tubulin post-translational modifications may contribute to the assembly of manchette and axoneme microtubules but also impact on IMT and IFT cargo transport by recruiting motor and non-motor proteins to ensure cargo delivery to specific intracellular sites in a developmental dependent manner. The sequential development of first the acrosome-acroplaxome complex and then the manchette, combined with the presence of proteins with cytoskeletal and vesicle binding affinity, suggest a precise developmental timing in cargo delivery. IMT and IFT require the participation of microtubule-associated proteins, including members of the kinesin and cytoplasmic dynein family and members of the IFT protein family.<sup>8</sup> Observations in two mutant mouse models, *azh* and *Ift88*, point to the significance of cargo transport along microtubule tracks in spermatids. As already indicated, spermatids express Hook1, a protein with known binding affinity to microtubules and vesicles.<sup>9</sup> This function may be compromised in the *azh* mutant mouse expressing truncated Hook1. How Hook1, alone or in combination with other microtubule-associated proteins, operates along microtubule tracks is not known. Spermatids of the *Ift88* mutant form a short and bulged tail containing randomly distributed microtubules and patches of unassembled outer dense fiber material. Vesicle cargo accumulates in the manchette.<sup>8</sup> A hypomorphic mutation of the *Ift88* gene impairs cargo transport also necessary for the development of primary cilia.<sup>47</sup> Whether IFT88 associates with the coiled-coil domains of Hook1 or GMAP210, as IFT20 does with a domain in the coiled-coil region of GMAP210,<sup>26</sup> remains to be determined.



The *azh* and *Ift88* mutant mouse models provide support to the hypothesis that defective IMT and IFT pathways contribute to the overall morphologies in spermatids. However, direct experimental evidence should determine how cargos are transported with the participation of motor and non-motor proteins. Biochemical studies highlight the abundance of post-translationally modified tubulin in fractionated manchettes,<sup>48</sup> but new high resolution technical approaches combined with differential sensitivity to drug- and cold-induced depolymerization are required to determine the distribution of subpopulations of microtubules in the manchette. The molecular properties of non-motor proteins such as GMAP210, IFT88 and Hook1 can be studied in

vitro using manchettes fractionated from wild-type and mutant mice. Alternatively, single molecule imaging can monitor the displacement of fluorescently labeled motor and non-motor proteins along cytoskeletal tracks in the cytoplasm of living spermatids. Understanding how motor and non-motor proteins interact with a subset of microtubules marked by post-translational modifications could clarify the origin of several phenotypic sperm abnormalities associated with male infertility.

#### Acknowledgments

This work was supported in part by NIH; grant numbers HD36477 and HD37282.

#### References

- Kierszenbaum AL. Intramanchette transport (IMT): managing the making of the spermatid head, centrosome and tail. *Mol Reprod Dev* 2002; 63:1-4.
- Goetz SC, Anderson KW. The primary cilium: a signaling centre during vertebrate development. *Nat Rev Genet* 2010; 11:331-44.
- Kierszenbaum AL, Rivkin E, Tres LL. Acroplaxome, an F-actin-keratin-containing plate, anchors the acrosome to the nucleus during shaping of the spermatid head. *Mol Biol Cell* 2003; 14:4628-40.
- Kierszenbaum AL, Tres LL, Rivkin E, Kang-Decker N, van Deursen JMA. The acroplaxome is the docking site of Golgi-derived myosin Va/Rab27a/b-containing proacrosomal vesicles in wild-type and Hrb mutant mouse spermatids. *Biol Reprod* 2004; 70:1400-10.
- Kierszenbaum AL, Rivkin E, Tres LL. The actin-based motor myosin Va is a component of the acroplaxome, an acrosome-nuclear envelope junctional plate, and of manchette-associated vesicles. *Cytogenet Genome Res* 2003; 103:337-44.
- Clermont Y, Oko R, Hermo L. Cell biology of mammalian spermiogenesis. In: Desjardins C, Ewing LL, Editors. *Cell and molecular biology of the testis*. New York: Oxford University Press 1993; 332-76.
- Göb E, Schmitt J, Benavente R, Alsheimer M. Mammalian sperm head formation involves different polarization of two novel LINC complexes. *PLoS One* 2010; 5:12072.
- Kierszenbaum AL, Rivkin E, Tres LL, Yoder BK, Haycraft CJ, Bornens M, Rios RM. GMAP210 and IFT88 are present in the spermatid Golgi apparatus and participate in the development of the acrosome-acroplaxome complex, head-tail coupling apparatus and tail. *Dev Dyn* 2011; 240:723-36.
- Mendoza-Lujambio I, Burfeind P, Dixkens C, Meinhardt A, Hoyer-Fender S, Engel W, Neesen J. The Hook1 gene is non-functional in the abnormal spermatozoon head shape (*azh*) mutant mouse. *Hum Mol Genet* 2002; 11:1647-58.
- Kierszenbaum AL, Gil M, Rivkin E, Tres LL. Ran, a GTP-binding protein involved in nucleocytoplasmic transport and microtubule nucleation, relocates from the manchette to the centrosome region during rat spermiogenesis. *Mol Reprod Dev* 2002; 63:131-40.
- Rivkin E, Tres LL, Kierszenbaum AL. Genomic origin, processing and developmental expression of testicular outer dense fiber 2 (ODF2) transcripts and a novel nucleolar localization of ODF2 protein. *Mol Reprod Dev* 2008; 75:1591-606.
- Rivkin E, Kierszenbaum AL, Gil M, Tres LL. Rnf19a, a ubiquitin protein ligase and Psmc3, a component of the 26S proteasome, tether to the acrosome membranes and the head-tail coupling apparatus during rat spermatid development. *Dev Dyn* 2009; 238:1851-61.
- Hammond JW, Cai D, Verhey KJ. Tubulin modifications and their cellular functions. *Curr Opin Cell Biol* 2008; 20:71-6.
- Moreno RD, Schatten G. Microtubule configurations and post-translational alpha-tubulin modifications during mammalian spermatogenesis. *Cell Motil Cytoskeleton* 2000; 46:235-46.
- Yang WX, Sperry AO. C-terminal kinesin motor KIF1C1 participates in acrosome biogenesis and vesicle transport. *Biol Reprod* 2003; 69:1719-29.
- Rios RM, Tassin AM, Celati C, Antony C, Boissier MC, Homberg JC, Bornens M. A peripheral protein associated with the cis-Golgi network redistributes in the intermediate compartment upon Brefeldin A treatment. *J Cell Biol* 1994; 125:997-1013.
- Rios RM, Sanchis A, Tassin AM, Feedriani C, Bornens M. GMAP-210 recruits gamma-tubulin complexes to cis-Golgi membranes and is required for Golgi ribbon formation. *Cell* 2004; 118:323-35.
- Yadav S, Puri S, Linstedt AD. A primary role for Golgi positioning in directed secretion, cell polarity and wound healing. *Mol Biol Cell* 2009; 20:1728-36.
- Infante C, Ramos-Morales F, Fedriani C, Bornens M, Rios RM. GMAP210, A cis-Golgi network-associated protein, is a minus end microtubule-binding protein. *J Cell Biol* 1999; 145:83-98.
- Kim HS, Takahashi M, Matsuo K, Ono Y. Recruitment of CG-NAP to the Golgi apparatus through interaction with dynein-dynactin complex. *Genes Cells* 2007; 12:421-34.
- Gillingham AK, Tong AH, Boone C, Munro S. The GTPase Arf1p and the ER to Golgi cargo receptor Erv14p cooperate to recruit the golgin Rud3p to the cis-Golgi. *J Cell Biol* 2004; 167:281-92.
- Drin G, Morello V, Casella JF, Gounon P, Antony B. Asymmetric tethering of flat and curved membranes by a golgin. *Science* 2008; 320:670-3.
- Kierszenbaum AL, Rivkin E, Tres LL. Expression of Fer testis (FerT) tyrosine kinase transcript variants and distribution sites of FerT during the development of the acrosome-acroplaxome-manchette complex in rat spermatids. *Dev Dyn* 2008; 237:3882-91.
- Kierszenbaum AL, Rivkin E, Talmor-Cohen A, Shalgi R, Tres LL. Expression of full-length and truncated Fyn tyrosine kinase transcripts and encoded proteins during spermatogenesis and localization during acrosome biogenesis and fertilization. *Mol Reprod Dev* 2009; 76:832-43.
- Sironen A, Hansen J, Thomsen B, Andersson M, Vilkkii J, Toppari J, Kotaja N. Expression of SPEF2 during mouse spermatogenesis and identification of IFT20 as an interacting protein. *Biol Reprod* 2010; 82:580-90.
- Follit JA, San Agustín JT, Xu F, Jonassen JA, Samtani R, Lo CW, Pazour GJ. The golgin GMAP210/TRIP11 anchors IFT20 to the Golgi complex. *PLoS Genet* 2008; 4:1000315.
- Moreno RD, Palomino J, Schatten G. Assembly of spermatid acrosome depends on microtubule organization during mammalian spermiogenesis. *Dev Biol* 2006; 293:218-27.
- Shubeita GT, Tran SL, Xu J, Vershinin M, Cermelli S, Cotton SL, et al. Consequences of motor copy number on the intracellular transport of kinesin-1-driven lipid droplets. *Cell* 2008; 135:1098-107.
- Ali MY, Kremontsova EB, Kennedy GG, Mahaffy R, Pollard TD, Trybus KM, Warsaw DM. Myosin Va maneuvers through actin intersections and diffuses along microtubules. *Proc Natl Acad Sci USA* 2007; 104:4332-6.
- Kierszenbaum AL, Tres LL. The acrosome-acroplaxome-manchette complex and the shaping of the spermatid head. *Arch Histol Cytol* 2004; 67:271-84.
- Daly RJ. Cortactin signalling and dynamic actin networks. *Biochem J* 2004; 382:13-25.
- Kai M, Irie M, Okutsu T, Inoue K, Ogonuki N, Miki H, et al. The novel dominant mutation Dspd leads to a severe spermiogenesis defect in mice. *Biol Reprod* 2004; 70:1213-21.
- Greer P. Closing in on the biological functions of Fps/Fes and Fer. *Nat Rev Mol Cell Biol* 2002; 3:278-89.
- Fouquet J, Kann M, Souès S, Melki R. ARP1 in Golgi organisation and attachment of manchette microtubules to the nucleus during mammalian spermatogenesis. *J Cell Sci* 2000; 113:877-86.
- Heid H, Figge U, Winter S, Kuhn C, Zimbelmann R, Franke W. Novel actin-related proteins Arp-T1 and Arp-T2 as components of the cytoskeletal calyx of the mammalian sperm head. *Exp Cell Res* 2002; 279:177-87.
- Hisano M, Yamada S, Tanaka H, Nishimune Y, Nozaki M. Genomic structure and promoter activity of the testis haploid germ cell-specific intronless genes, Tact1 and Tact2. *Mol Reprod Dev* 2003; 65:148-56.
- Tanaka H, Iguchi N, Egidio de Carvalho C, Tadokoro Y, Yomogida K, Nishimune Y. Novel actin-like proteins T-ACTIN 1 and T-ACTIN 2 are differentially expressed in the cytoplasm and nucleus of mouse haploid germ cells. *Biol Reprod* 2003; 69:475-82.
- Chadwick BP, Mull J, Helbling LA, Gill S, Leyne M, Robbins CM, et al. Cloning, mapping and expression of two novel actin genes, actin-like-7A (ACTL7A) and actin-like-7B (ACTL7B), from the familial dysautonomia candidate region on 9q31. *Genomics* 1999; 58:302-9.
- Hurst S, Howes EA, Coadwell J, Jones R. Expression of a testis-specific putative actin-capping protein associated with the developing acrosome during rat spermiogenesis. *Mol Reprod Dev* 1998; 49:81-91.
- Coutts AS, MacKenzie E, Griffith E, Black DM. TES is a novel focal adhesion protein with a role in cell spreading. *J Cell Sci* 2003; 116:897-906.
- Behnen M, Murk K, Kursula P, Cappallo-Obermann H, Rothkegel M, Kierszenbaum AL, Kirchhoff C. Testis-expressed profilins 3 and 4 show distinct functional characteristics and localize in the acroplaxome-manchette complex in spermatids. *BMC Cell Biol* 2009; 10:34.
- Kramer H, Phistry M. Genetic analysis of hook, a gene required for endocytic trafficking in *Drosophila*. *Genetics* 1999; 675-84.

43. Mochida K, Tres LL, Kierszenbaum AL. Structural and biochemical features of fractionated spermatid manchettes and sperm axonemes of the *azh/azh* mutant mouse. *Mol Reprod Dev* 1999; 52:434-44.
44. Schroer TA. Dynactin. *Annu Rev Cell Dev Biol* 2004; 20:759-79.
45. Hall ES, Eveleth J, Jiang C, Redenbach DM, Boekelheide K. Distribution of the microtubule-dependent motors cytoplasmic dynein and kinesin in rat testis. *Biol Reprod* 1992; 46:817-28.
46. Kierszenbaum AL. Sperm axoneme: a tale of tubulin posttranslation diversity. *Mol Reprod Dev* 2002; 62:1-3.
47. Lehman JM, Michaud EJ, Schoeb TR, Aydin-Sun Y, Miller M, Yoder BK. The Oak Ridge Polycystic kidney mouse: Modeling ciliopathies of mice and men. *Dev Dyn* 2008; 237:1960-71.
48. Mochida K, Tres LL, Kierszenbaum AL. Isolation of the rat spermatid manchette and its perinuclear ring. *Dev Biol* 1998; 200:46-56.
49. Rivkin E, Cullinan EB, Tres L, Kierszenbaum AL. A protein associated with the manchette during rat spermiogenesis is encoded by a gene of the TBP-1-like subfamily with highly conserved ATPase and protease domains. *Mol Reprod Dev* 1997; 48:77-89.